NFN - Nationales Forschungsnetzwerk

Geometry + Simulation

http://www.gs.jku.at

Lofting with Patchwork B-splines

Nora Engleitner, Bert Jüttler

G+S Report No. 79

February 2019

Der Wissenschaftsfonds.

JOHANNES KEPLER UNIVERSITY LINZ

Lofting with Patchwork B-splines

Nora Engleitner, Bert Jüttler

Abstract Lofting – also denoted as surface skinning – is one of the fundamental operations for creating free-form surfaces in Computer Aided Design. This process generates a surface from a given sequence of section curves. It is particularly useful for airfoils and turbine blades, since these shapes are often defined by cross sections with a family of auxiliary surfaces. The use of tensor-product B-splines, which is currently the standard technology, leads to large data volumes if section curves with incompatible knot vectors are used. We adopt the framework of Patchwork B-splines, which supports very flexible refinement strategies, and apply it to the construction of lofting surfaces. This approach not only reduces the resulting data volume but also limits the propagation of derivative discontinuities.

Key words: tensor-product B-splines, Patchwork B-splines, adaptive refinement, lofting, surface skinning

1 Introduction

The process of lofting, which is also called surface skinning, is one of the fundamental operations for the construction of free-form surfaces in geometric design, and its origins can be traced back to the early days for Computer-Aided Design [14]. It creates surfaces from given sequences of section curves, and it is particularly useful for airfoils and turbine blades, since these shapes are often defined by cross sections with a family of auxiliary surfaces.

More precisely, we consider a sequence of space curves $c_k(u)$, $k = 0, \ldots, N$, which are all defined over the parameter interval $[0,1]$. Each curve is represented as B-spline curve of degree p_k,

Johannes Kepler University, Institute of Applied Geometry, Linz / Austria
e-mail: nora.engleitner@jku.at, bert.juettler@jku.at

$$c_k(u) = \sum_{i=0}^{m_k} d_{i,k} N_{i,p_k,T_k}(u), \quad \text{for } k = 0, \ldots, N,$$

with control points $d_{i,k} \in \mathbb{R}^3$ and B-splines N_{i,p_k,T_k} of degree p_k defined on the knot vector T_k. These curves will be denoted as *section curves*, since they represent the intersection of an unknown surface (the lofting surface) with a family of auxiliary surfaces. Note that the degrees and the knot vectors are potentially different for each of the section curves.

A lofting surface $s(u,v)$ is a surface with parameter domain $[0,1]^2$, that interpolates the section curves at certain parameters $\bar{v}_k$, i.e.,

$$s(u, \bar{v}_k) = c_k(u), \quad \text{for all } k = 0, \ldots, N.$$

This paper is devoted to procedures that generate a lofting surface from the given section curves.

The construction of lofting surfaces has been analyzed in a substantial number of publications. In order to keep the paper focused, we list only a few representative references.

The basic definition and construction of tensor-product B-spline lofting surfaces via interpolation of spline curves is described by Piegl and Tiller [11]. The same authors also introduced an approximate approach [10], which helps to reduce the required data volume. In fact, the number of control points of tensor-product spline lofting surfaces will be quite large if the section curves possess incompatible knot vectors, and this motivates the use of approximate methods. In another paper, they presented several improvements and extensions of the skinning algorithm [12].

In recent years, research has focused on particular geometric problems related to skinning and lofting. Bizzarri et al. [1] describe techniques for skinning and blending with rational envelope surfaces. Kunkli and Hoffmann [8] discuss the skinning of sequences of circles and spheres.

Besides tensor-product spline spaces, it appears to be promising to use spline spaces that support adaptive refinement. As one of the first contributions in this direction, Yang and Zhen [15] applied the T-spline technology to perform approximate surface skinning. Li et al. [9] provide an explicit method for surface skinning using periodic T-spline surfaces.

Hierarchical splines [7] are another well-established approach to adaptive refinement of tensor-product splines. Recently, the original construction of a basis was enhanced by introducing the truncation mechanism [4, 5]. This has prepared the ground for the definition of Patchwork B-splines (PB-splines), which form a generalization of hierarchical splines that provides further possibilities for adaptive refinement [3].

The present paper applies this new construction of adaptive splines to the construction of lofting surfaces. We are able to perform exact interpolation of the section curves and obtain a smaller data volume than tensor-product spline lofting surfaces. Moreover, the use of PB-splines also helps to limit the propagation of derivative discontinuities. In addition, the construction is very flexible, supporting not only knot vectors containing knots with varying multiplicities, but even section curves with different polynomial degrees.

The remainder of the paper is structured into five sections. The next section recalls the standard approach, which employs tensor-product splines, based on the technology described in [11]. Section 3 introduces a very simple blending-based solution, which is not useful for applications but helps to prove the existence of PB-spline lofting surfaces. The fourth section adapts PB-splines to the lofting problem and describes the new method for lofting. Several computational results are presented in Section 5, in order to compare the tensor-product B-spline and PB-spline lofting surfaces. Finally, we conclude the paper.

2 Lofting with tensor-product B-splines

We construct a tensor-product B-spline surface of degree (p,q) with knot vectors U and V,

$$s_{\mathrm{tp}}(u,v) = \sum_{i=0}^{m}\sum_{j=0}^{n} c_{i,j} N_{i,p,U}(u) N_{j,q,V}(v),$$

that interpolates the section curves $c_k(u)$ of degrees p_k with knot vectors T_k, i.e.,

$$\sum_{i=0}^{m}\sum_{j=0}^{N} c_{i,j} N_{i,p,U}(u) N_{j,q,V}(\bar{v}_k) = \sum_{i=0}^{m_k} d_{i,k} N_{i,p_k,T_k}(u), \quad \text{for all } k = 0,\ldots,N.$$

In order to generate such a tensor-product spline surface, we create a knot vector U defining a spline space of degree

$$p = \max_{k=0,\ldots,N} p_k,$$

which contains the spline spaces associated with the section curves. Consequently, each section curve possesses a representation

$$c_k(u) = \sum_{i=0}^{m} d^{\star}_{i,k} N_{i,p,U}(u), \quad \text{for } k = 0,\ldots,N. \tag{1}$$

In addition, we choose a suitable degree q, the parameters $\bar{v}_k$ and a corresponding knot vector $V = \{v_i\}_{i=0,\ldots,N+q+1}$. Finally, we apply a curve interpolation algorithm to the rows of control points $d^{\star}_{i,0},\ldots,d^{\star}_{i,N}$, to compute the control points $c_{i,j}$ of the lofting surface. More precisely, $c_{i,j}$ is the j-th control point of the B-spline curve that interpolates the points $d^{\star}_{i,0},\ldots,d^{\star}_{i,N}$.

Now we discuss the procedure in more detail, summarizing the approach presented in [11]. We start by constructing the common knot vector U. First, we have to perform degree elevation on the curves until all curves have the same degree p. Second, we apply the knot insertion algorithm to the different, degree elevated knot vectors until we arrive at the common knot vector U with basis functions $N_{i,p,U}$, $i = 0,\dots,m$, for all curves. Hence, we construct U as the union of all knots, with associated multiplicities, that appear in one of the knot vectors T_k after the degree elevation. The knot insertion algorithm also provides the new control points $d^\star_{i,k}$ of the curves in (1), such that the shape of the section curves is preserved.

Next we have to choose a degree q, compute the parameters $\bar{v}_k$ and define a knot vector V in v-direction. The degree can be chosen freely as long as it satisfies $q \le N$. For computing the parameters $\bar{v}_k$ and the knots $v_i \in V$ we use an averaging approach based on chord-length parameterization. The parameters $\bar{v}_k$ are chosen as

$$\bar{v}_0 = 0, \quad \bar{v}_N = 1$$

and

$$\bar{v}_k = \bar{v}_{k-1} + \frac{1}{m+1} \sum_{i=0}^{m} \frac{|d^\star_{i,k} - d^\star_{i,k-1}|}{L_i}, \quad \text{for } k = 1,\dots,N-1,$$

with $L_i = \sum_{k=1}^{N} |d^\star_{i,k} - d^\star_{i,k-1}|$. The knots v_i are obtained by averaging the parameter values,

$$v_0 = \ldots = v_q = 0, \quad v_{N+1} = \ldots = v_{N+q+1} = 1$$

and

$$v_i = \frac{1}{q} \sum_{k=i-q}^{i-1} \bar{v}_k, \quad \text{for } i = q+1,\dots,N.$$

Finally we compute the control points $c_{i,j}$ for $i = 0,\dots,m$ and $j = 0,\dots,n$. Interpolating over the rows of control points $d^\star_{i,0},\dots,d^\star_{i,N}$ results in $m+1$ systems of equations with $N+1$ unknowns each. More precisely, for all $i = 0,\dots,m$ we solve the $N+1$ equations

$$\sum_{j=0}^{n} c_{i,j} N_{j,q,V}(\bar{v}_k) = d^\star_{i,k}, \quad \text{for } k = 0,\dots,N,$$

for the $N+1$ control points $c_{i,j}$ with $j = 0,\dots,N$. As stated in [11], the choice of parameters and knots v_i guarantees that the systems are regular.

The method can be generalized by considering larger knot vectors V, which provide additional degrees of freedom. These degrees of freedom can be used to satisfy additional constraints or to optimize the shape of the resulting lofting surfaces. Our experimental results are based on the implementation in the Parasolid™ CAD kernel.

Generating a lofting surface with tensor-product B-splines is a relatively simple but highly effective tool and is therefore used in virtually all CAD systems. However, as a consequence of the degree elevation and knot insertion, the resulting surface may possess a considerable number of control points, especially when using a large number of section curves or curves with different knots and varying degrees.

3 Blending-based lofting

A particularly simple solution to the lofting problem can be obtained by the blending approach. This approach is not based on a globally defined tensor-product spline space, hence it provides a coarse representation of the lofting surface.

We define blending B-spline functions,

$$B_i(v) = \sum_{r=0}^{q} N_{i(q+1)+r,q,V}(v),$$

for $i = 0,\ldots,N$. The corresponding lofting surface is then defined as

$$s_{\text{blend}}(u,v) = \sum_{k=0}^{N} c_k(u) B_k(v).$$

Again we have to determine the degree q, the parameters $\bar{v}_k$ and the knot vector V. As in the previous section, the degree q can be choosen arbitrarily. The parameters are computed with an averaging proceedure similar to the tensor-product B-spline case. However, we do not compute the distances between the control points here, since we do not have a one-to-one correspondence between the control points of adjacent section curves. Instead we use sample points on the section curves to obtain the parameter values $\bar{v}_k$. Hence, we evaluate all curves at the parameter values

$$r_i = \frac{i}{\hat{m}}, \quad \text{for } i = 0,\ldots,\hat{m}, \quad \hat{m} = \max_{k=0,\ldots,N} m_k,$$

and compute the parameters as

$$\bar{v}_0 = 0, \quad \bar{v}_N = 1 \tag{2}$$

and

$$\bar{v}_k = \bar{v}_{k-1} + \frac{1}{\hat{m}+1} \sum_{i=0}^{\hat{m}} \frac{|c_k(r_i) - c_{k-1}(r_i)|}{\hat{L}_i} \tag{3}$$

with

$$\hat{L}_i = \sum_{k=1}^{N} |c_k(r_i) - c_{k-1}(r_i)|.$$

We define the knots $v_i \in V$ such that each parameter $\bar{v}_k$ is contained in the knot span $[v_{i_k}, v_{i_k+1}]$ and that v_{i_k+1} and $v_{i_{k+1}}$ are separated by q knot spans. To be more precise, we choose the the first and last $q+1$ knots as

$$v_0 = \ldots = v_q = 0, \quad \text{and} \quad v_{n-q} = \ldots = v_n = 1, \tag{4}$$

with $n = (N+2)(q+1)$. The remaining knots are then defined as

$$v_{k(q+1)+i} = \begin{cases} \bar{v}_{k-1} + (i+1)h_k, & \text{if } k = 1, \\ \bar{v}_{k-1} + (i+\frac{1}{2})h_k, & \text{else,} \end{cases} \tag{5}$$

with

$$h_k = \begin{cases} \frac{\bar{v}_k - \bar{v}_{k-1}}{q+\frac{3}{2}}, & \text{if } k = 1 \text{ or } k = N, \\ \frac{\bar{v}_k - \bar{v}_{k-1}}{q+1}, & \text{else,} \end{cases}$$

for $k = 1, \ldots, N$ and $i = 0, \ldots, q$. Figure 1 shows an example of a lofting surface obtained by this simple blending approach. As an advantage, the lofting surface is obtained without the need for solving systems of linear equations. However, the section curves correspond to singular curves on the lofting surface. Clearly, the quality of this result is not sufficient for applications. Nevertheless, we will use the blending approach to prove the existence of solutions for the lofting surface defined by PB-splines.

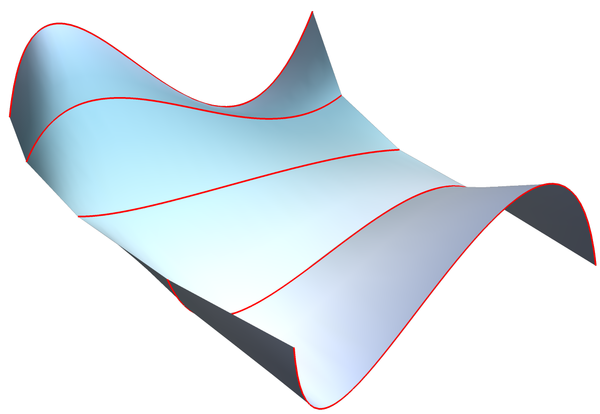

Fig. 1 Example for a blending-based lofting surface over 5 section curves (colored in red).

4 Lofting with PB-splines

After discussing tensor-product B-spline and the blending-based lofting, we introduce a novel lofting method that provides high-quality surfaces while keeping the number of degrees of freedom small. The construction is based on Patchwork B-splines (PB-splines) that are defined on sequences of partially nested tensor-product spline spaces with associated patches. This enables us to employ independently chosen spline spaces in the vicinity of the section curves, thereby eliminating redundant control points.

4.1 Patchwork B-splines

We recall the definion of Patchwork B-splines via a patchwork hierarchy that defines a patchwork spline space. PB-splines are defined by suitably generalizing the selection mechanism for hierarchical B-splines. We present certain assumptions on the patchwork hierarchy which guarantee linear independence and that the PB-splines form a basis for the patchwork spline space.

The patchwork hierarchy

The patchwork hierarchy combines a sequence of tensor-product spline spaces with a corresponding sequence of patches.

First, we consider a finite sequence of spline spaces S^ℓ that are spanned by tensor-product B-splines,

$$S^\ell = \operatorname{span}\{N_{i,p_\ell,U_\ell}\, N_{j,q_\ell,V_\ell}\}_{(i,j)\in\mathscr{J}^\ell},$$

for the *levels* $\ell = 0,\dots,2N$ with the index set

$$\mathscr{J}^\ell = \{(i,j) \;:\; i = 0,\dots,m_\ell,\; j = 0,\dots,n_\ell\}.$$

The basis functions are defined over knot vectors U_ℓ and V_ℓ of degrees p_ℓ and q_ℓ in u- and v-direction, respectively. At a point $\mathbf{x} = (u,v)$, the basis functions possess the smoothness

$$\mathbf{s}^\ell(\mathbf{x}) = (s_1^\ell(u), s_2^\ell(v)) = (p_\ell - m_1^\ell(u), q_\ell - m_2^\ell(v)),$$

where $m_1^\ell(u)$ is the multiplicity of u in U_ℓ and $m_2^\ell(v)$ the multiplicity of v in V_ℓ. Note that the spline spaces S^ℓ are not required to be nested, i.e., S^ℓ is not necessarily a subspace of $S^{\ell+1}$.

Second, we assign a corresponding *patch* π^ℓ to every spline space S^ℓ. The patches are mutually disjoint open rectangles in the $\mathbb{R}^2$ that cover the *domain* Ω,

$$\Omega = \bigcup_{\ell=0}^{2N} \overline{\pi^\ell} = [0,1]^2.$$

Furthermore, we assume that the boundaries of a patch π^ℓ are aligned with the knot lines of the corresponding spline space. [1]

Finally, we introduce the *patchwork spline space* P, which contains functions $f \in C([0,1]^2)$ with the follwing two properties.

(i) The restriction of f to one of the patches is contained in the corresponding spline space on that patch, i.e.,

---

[1] Note that the PB-spline construction defined in [3] allows arbitrary domains and admits more general open subsets of the $\mathbb{R}^d$ as patches. However, for the lofting problem this simpler setting is sufficient.

$$f|_{\pi^\ell} \in S^\ell|_{\pi^\ell}, \quad \text{for } \ell = 0, \ldots, 2N.$$

(ii) The restriction of f to $\overline{(\pi^\ell \cap \pi^k)}$ possesses the smoothness $\mathbf{s}^{\max(\ell,k)}(\mathbf{x})$ for all $\mathbf{x} \in \overline{\pi^\ell} \cap \overline{\pi^k}$.

Clearly, the properties of the functions in the patchwork spline space are determined by the chosen patchwork hierarchy, i.e., by the sequence of tensor-product spline spaces and associated patches.

The selection mechanism

In order to construct a basis for the patchwork spline space we adapt Kraft's selection mechanism [7], which is based on the relation between the support of a B-spline and certain subdomains. Instead of this classical approach, we work with the constraining boundary Γ^ℓ of a patch π^ℓ, which is defined as the part of the boundary $\partial\pi^\ell$ that is shared with patches of a lower level,

$$\Gamma^\ell = \bigcup_{k=0}^{\ell-1} \overline{\pi^k} \cap \overline{\pi^\ell}.$$

We use a constraining boundary–based selection mechanism on the patchwork hierarchy to obtain a basis. For each level ℓ we select the bivariate basis functions $N_{i,p_\ell,U_\ell}\, N_{j,q_\ell,V_\ell}$ that are active on the corresponding patch π^ℓ while vanishing at the constraining boundary Γ^ℓ,

$$\mathscr{K}^\ell = \{(i,j) \in \mathscr{J}^\ell \,:\, (N_{i,p_\ell,U_\ell}\, N_{j,q_\ell,V_\ell})|_{\pi^\ell} \neq 0 \text{ and } (N_{i,p_\ell,U_\ell}\, N_{j,q_\ell,V_\ell})|_{\Gamma^\ell} = 0\} \quad (6)$$

The supports of the selected basis functions of level ℓ define the *shadow* $\hat{\pi}^\ell$ of a patch,

$$\hat{\pi}^\ell = \bigcup_{(i,j)\in\mathscr{K}^\ell} \operatorname{supp}(N_{i,p_\ell,U_\ell}\, N_{j,q_\ell,V_\ell}), \quad \ell = 0, \ldots, 2N.$$

Finally, collecting the selected basis functions from all levels gives us the *Patchwork B-splines* (PB-splines),

$$K = \bigcup_{\ell=0}^{2N} \{(N_{i,p_\ell,U_\ell}\, N_{j,q_\ell,V_\ell}) \,:\, (i,j) \in \mathscr{K}^\ell\}.$$

Linear independence and space characterization

Two assumptions allow us to characterize the space that is spanned by the PB-splines:

Assumption S2C. The patches and spline spaces possess the property of *Simple Shadow Compatibility*:

(i) The shadow $\hat{\pi}^\ell$ of a patch π^ℓ does not intersect patches of a lower level $k < \ell$, i.e.,

$$\hat{\pi}^\ell \cap \pi^k = \emptyset, \quad \text{for all } k < \ell.$$

(ii) If the shadow $\hat{\pi}^k$ of a level $k < \ell$ intersects the patch π^ℓ then the corresponding spaces are nested, i.e.,

$$\hat{\pi}^k \cap \pi^\ell \neq \emptyset \implies S^k \subseteq S^\ell, \quad \text{for all } k < \ell.$$

Assumption SMC. All patches and associated spline spaces fulfill the *Smoothness Monotonicity Condition*: The smoothness across the constraining boundary Γ^ℓ in transversal direction does not increase when moving from a lower to a higher level, i.e., for $k < \ell$ it holds that

$$s_i^\ell(\mathbf{x}) \leq s_i^k(\mathbf{x}) \qquad \text{for all} \quad \mathbf{x} \in \Gamma^\ell \cap \overline{\pi^k},$$

where the i-th coordinate direction is transversal with respect to Γ^ℓ at $\mathbf{x}$.

As shown in [3], these two assumptions imply two fundamental results:

Theorem 1. *The PB-splines are linearly independent on Ω if the patchwork hierarchy satisfies Assumption S2C.*

Consequently, the selected B-splines from all levels form a basis.

Theorem 2. *The PB-splines span the patchwork spline space P if Assumptions S2C and SMC are both satisfied.*

Therefore, we have two different characterizations of the patchwork spline space P. On the one hand, there is the implicit definition that characterizes the space by the properties of the functions it contains. On the other hand, we have a constructive definition that describes P as the linear hull of its basis, namely the PB-splines.

Note, that the PB-splines do not form a partition of unity. In order to restore this property we have to introduce a truncation mechanism [3]. A detailed discussion is beyond the scope of the present paper.

4.2 The patchwork hierarchy for lofting

Recall that we want to construct a PB-spline surface $s_{\mathrm{pb}}(u,v)$, which satisfies the interpolation conditions $s_{\mathrm{pb}}(u,\bar{v}_k) = c_k(u)$ for certain parameter values $\bar{v}_0,\ldots,\bar{v}_N$, i.e.,

$$s_{\mathrm{pb}}(u,\bar{v}_k) = \sum_{\ell=0}^{2N} \sum_{(i,j)\in\mathscr{K}^\ell} c_{i,j}^\ell N_{i,p_\ell,U_\ell}(u) N_{j,q_\ell,V_\ell}(\bar{v}_k) = \sum_{i=0}^{m_k} d_{i,k} N_{i,p_k,T_k}(u),$$

for $k = 0, \ldots, N$. We choose the same spline space in v-direction for all levels, i.e., $V_\ell = V$ and $q_\ell = q$. The degree, the parameter values $\bar{v}_k$ and the elements of the knot vector $V = \{v_i\}$ are chosen in the same way as for the blending-based loft. Consequently, the locations of the parameters $\bar{v}_0, \ldots, \bar{v}_N$ are determined by (2) and (3), and the knots v_i take the values (4) and (5). How to construct the vectors U_ℓ will be discussed later.

Curve patches and intermediate patches

All patches are chosen as axis-aligned boxes. We denote the southwest (lower left) and northeast (upper right) vertex of the rectangular patch π^ℓ by

$$\mathbf{r}_{\mathrm{sw}}^\ell = (r_{\mathrm{sw},1}^\ell, r_{\mathrm{sw},2}^\ell) \quad \text{and} \quad \mathbf{r}_{\mathrm{ne}}^\ell = (r_{\mathrm{ne},1}^\ell, r_{\mathrm{ne},2}^\ell),$$

respectively. The first $N+1$ patches possess the vertices

$$\mathbf{r}_{\mathrm{sw}}^\ell = (0, v_{(\ell+1)(q+1)-1}) \quad \text{and} \quad \mathbf{r}_{\mathrm{ne}}^\ell = (1, v_{(\ell+1)(q+1)}), \tag{7}$$

for $\ell = 0, \ldots, N$. We denote these patches as *curve patches* since each of them contains the parameter value which is associated with one of the section curves,

$$(0,1) \times \{\bar{v}_\ell\} \subset \pi^\ell .$$

Consecutive curve patches π^ℓ and $\pi^{\ell+1}$ are connected by the *intermediate patch* $\pi^{\ell+N+1}$ with the vertices

$$\mathbf{r}_{\mathrm{sw}}^{\ell+N+1} = (0, r_{\mathrm{ne},2}^\ell) \quad \text{and} \quad \mathbf{r}_{\mathrm{ne}}^{\ell+N+1} = (1, r_{\mathrm{sw},2}^{\ell+1}),$$

for $\ell = 0, \ldots, N-1$.

Summing up, all the patches are horizontal stripes with width 1. The height of the curve patches is determined by a single knot span of the knot vector V, while the height of the intermediate patches is equal to q knot spans.

Now we discuss the choice of the knot vector U_ℓ and the associated degree p_ℓ for each patch. Again we distinguish between curve and intermediate patches.

The curve patch π^ℓ, $\ell = 0, \ldots, N$, simply inherits the degree p_ℓ and the knot vector T_ℓ from the corresponding section curve $c_\ell(u)$. The intermediate patch π^ℓ, $\ell = N+1, \ldots, 2N$, has the degree

$$p_\ell = \max\{p_{\ell-N-1}, p_{\ell-N}\}.$$

The corresponding knot vector is obtained by first applying degree elevation to the knot vectors $U_{\ell-N-1}$ and $U_{\ell-N}$ and then performing knot insertion until one arrives at a knot vector U_ℓ that is the union of the degree elevated knot vectors, where each knot is considered with multiplicity.

The resulting patchwork hierarchy, which is fully determined by the given section curves, will be denoted as H. Fig. 2 shows an instance of such a hierarchy for 5 section curves of maximum smoothness and degrees $p_k = q = 3$.

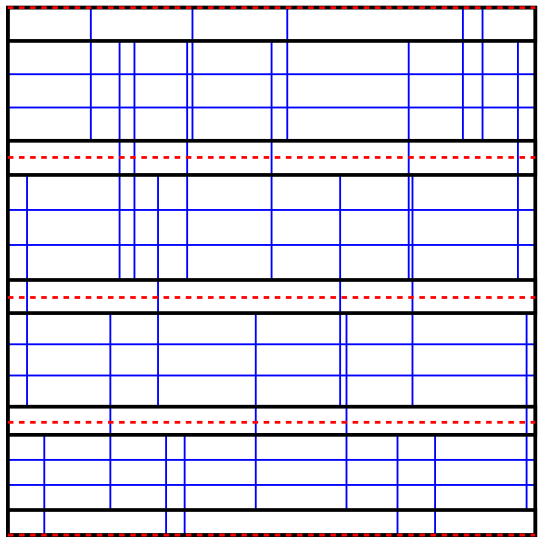

Fig. 2 Example for a simple patchwork hierarchy H. Blue lines represent the knot lines, black lines are patch boundaries and dashed red lines illustrate the parameter lines $v = \bar{v}_k$.

Basis construction

Applying the selection mechanism (6) to the patchwork hierarchy H generates sets of basis functions with associated index sets

$$\mathscr{K}^\ell = \{(i,j) \ : \ i = 0,\dots,m_\ell,\ j = \ell(q+1),\dots,(\ell+1)(q+1)-1\},$$

for $\ell = 0,\dots,N$ and

$$\mathscr{K}^\ell = \emptyset,$$

for $\ell > N$. In fact, we select $m_\ell(q+1)$ basis functions from each curve patch and none from the intermediate patches. The total number of selected functions is equal to

$$|K| = (q+1)\sum_{\ell=0}^{N} m_\ell.$$

Corollary 3. *The patchwork hierarchy H satisfies S2C and SMC.*

Proof. The shadow of a curve patch π^ℓ is an axis-aligned box with lower-left and upper-right corners

$$\hat{\mathbf{r}}^\ell_{\mathrm{sw}} = (0, v_{\ell(q+1)}) \quad \text{and} \quad \hat{\mathbf{r}}^\ell_{\mathrm{ne}} = (1, v_{(\ell+2)(q+1)-1}),$$

respectively. These vertices can be rewritten as

$$\hat{\mathbf{r}}^\ell_{\mathrm{sw}} = \begin{cases} (0,0), & \text{if } \ell = 0, \\ (0, r^{\ell-1}_{\mathrm{ne},2}), & \text{otherwise,} \end{cases} \quad \text{and} \quad \hat{\mathbf{r}}^\ell_{\mathrm{ne}} = \begin{cases} (1,1), & \text{if } \ell = N, \\ (1, r^{\ell+1}_{\mathrm{sw},2}), & \text{otherwise.} \end{cases}.$$

Thus, the shadow $\hat{\pi}^\ell$ extends only to the neighboring intermediate patches, which possess a level larger than ℓ. Moreover, the shadows of the intermediate patches are empty. The first part of S2C is therefore satisifed.

For the second part of S2C we note that the construction of the vectors U_ℓ implies that $S^{\ell-N-1} \subseteq S^\ell$ and $S^{\ell-N} \subseteq S^\ell$ for $\ell = N+1, \ldots, 2N$. Thus, S2C is fulfilled by the patchwork hierarchy H.

Now we consider SMC. Note that S2C implies SMC for all pairs of neighboring patches π^k and π^ℓ with $k < \ell$ and $\hat{\pi}^k \cap \pi^\ell \neq \emptyset$. Since no other pairs of neighboring patches exist in H, we conclude that SMC is also satisfied.

Theorem 4. *The Patchwork B-splines defined on H form a partition of unity,*

$$\sum_{k=0}^{2N} \sum_{(i,j)\in\mathscr{K}^k} N_{i,p_k,U_k}(u) N_{j,q,V}(v) = 1, \quad \textit{for } (u,v) \in \Omega. \tag{8}$$

Proof. Recall that the tensor-product B-splines $N_{i,p_\ell,U_\ell}\, N_{j,q,V}$ with $(i,j) \in \mathscr{J}^\ell$ form a partition of unity on $[0,1]^2$. We consider the restriction to π^ℓ and obtain

$$\sum_{\substack{(i,j)\in\mathscr{J}^\ell \\ (N_{i,p_\ell,U_\ell} N_{j,q,V})|_{\pi^\ell} \neq 0}} N_{i,p_\ell,U_\ell}(u) N_{j,q,V}(v) = 1, \quad \text{for } (u,v) \in \pi^\ell. \tag{9}$$

This summation considers the indices

$$\{(i,j) \,:\, i = 0,\ldots,m_\ell,\; j = \ell(q+1),\ldots,(\ell+1)(q+1)-1\} \tag{10}$$

for $\ell = 0, \ldots, N$ and

$$\{(i,j) \,:\, i = 0,\ldots,m_\ell,\; j = (\ell-N-1)(q+1)+1,\ldots,(\ell-N+1)(q+1)-2\} \tag{11}$$

for $\ell = N+1, \ldots, 2N$.

First, we show the partition of unity on a curve patch π^ℓ, with $\ell = 0, \ldots, N$. The left-hand side of (8) evaluates to

$$\sum_{k=0}^{2N} \sum_{(i,j)\in\mathscr{K}^k} N_{i,p_k,U_k}(u) N_{j,q,V}(v) = \sum_{(i,j)\in\mathscr{K}^\ell} N_{i,p_\ell,U_\ell}(u) N_{j,q,V}(v), \quad \text{for } (u,v) \in \pi^\ell.$$

Since the index set $\mathscr{K}^\ell$ coincides with the set in (10), the partition of unity is implied by (9).

Second, when considering the restriction to an intermediate patch π^ℓ, with $\ell = N+1,\ldots,2N$, we observe that the only functions that contribute to the sum on the left-hand side in (8) possess the indices

$$\bigcup_{k=\ell-N-1}^{\ell-N} \{(i,j) \in \mathscr{J}^k \,:\, (N_{i,p_k,U_k} N_{j,q,V})|_{\overline{\pi^k} \cap \overline{\pi^\ell}} \neq 0\}.$$

Therefore, this left-hand side can be rewritten as

$$\Big(\sum_{i=0}^{m_{\ell-N-1}} N_{i,p_{\ell-N-1},U_{\ell-N-1}}(u)\Big)\Big(\sum_{j=(\ell-N-1)(q+1)+1}^{(\ell-N)(q+1)-1} N_{j,q,V}(v)\Big) + \Big(\sum_{i=0}^{m_{\ell-N}} N_{i,p_{\ell-N},U_{\ell-N}}(u)\Big)\Big(\sum_{j=(\ell-N)(q+1)}^{(\ell-N+1)(q+1)-2} N_{j,q,V}(v)\Big), \quad \text{for } (u,v) \in \pi^\ell.$$

The two sums with index i are equal to one, according to the partition of unity property of univariate B-splines. Merging the remaining two sums confirms (8) on π^ℓ, since the summation with respect to j is in agreement with the index set defined in (11).

Since the selected B-splines defined by H satisfy S2C and SMC, they form a basis of the associated patchwork spline space according to Theorem 2. This fact enables us to obtain the following result.

Theorem 5. *The patchwork spline space P defined by the hierarchy H contains the coordinate functions of the lofting surface $s_{\text{blend}}(u,v)$, which is generated by the blending-based approach.*

Proof. We show that the restrictions of $s_{\text{blend}}(u,v)$ to the patches π^ℓ belong to the associated spline spaces S^ℓ. Recall that

$$s_{\text{blend}}(u,v) = \sum_{k=0}^{N}\sum_{i=0}^{m_k}\sum_{r=0}^{q} d_{i,k} N_{i,p_k,T_k}(u) N_{k(q+1)+r,q,V}(v).$$

First we consider a curve patch π^ℓ, $\ell = 0,\ldots,N$. We obtain

$$s_{\text{blend}}(u,v) = \sum_{i=0}^{m_\ell}\sum_{r=0}^{q} d_{i,\ell} N_{i,p_\ell,T_\ell}(u) N_{\ell(q+1)+r,q,V}(v), \quad \text{for } (u,v) \in \pi^\ell.$$

By comparing the knot vectors we find

$$s_{\text{blend}}(u,v) = \sum_{(i,j)\in\mathscr{K}^\ell} d_{i,\ell} N_{i,p_\ell,U_\ell}(u) N_{j,q,V}(v), \quad \text{for } (u,v) \in \pi^\ell,$$

which implies that the restriction of $s_{\text{blend}}(u,v)$ to the curve patch π^ℓ is contained in S^ℓ for $\ell = 0,\ldots,N$.

Second, for the intermediate patches π^ℓ, $\ell = N+1,\dots,2N$, we obtain

$$s_{\text{blend}}(u,v) = \sum_{k=\ell-N-1}^{\ell-N} \sum_{(i,j)\in\mathscr{K}^k} d_{i,k} N_{i,p_k,U_k}(u) N_{j,q,V}(v), \quad \text{for } (u,v)\in\pi^\ell.$$

Assumption S2C guarantees that

$$S^{\ell-N-1} \subseteq S^\ell \quad \text{and} \quad S^{\ell-N} \subseteq S^\ell, \tag{12}$$

which implies that the restriction of $s_{\text{blend}}(u,v)$ to the intermediate patch π^ℓ is contained in S^ℓ for $\ell = N+1,\dots,2N$.

In addition, we need to verify the smoothness property (ii). This follows immediately from (12) as well and completes the proof.

4.3 Comparison with other adaptive splines

For section curves of uniform degrees $p = p_\ell$, where $\ell = 0,\dots,N$, the basis constructed on the patchwork hierarchy H can equivalently be generated by other adaptive spline constructions. We focus on (analysis-suitable) T-splines and LR B-splines, e.g., see [13] and [2].

First, we consider T-splines on the T-mesh defined by horizontal lines with start points $(0,v_i)$ and end points $(1,v_i)$ for all knot values $v_i \in V$, where V is computed as for the PB-splines, and vertical lines with start and end points

$$(\omega, r^\ell_{\text{sw},2} - \lfloor \frac{q}{2} \rfloor) \quad \text{and} \quad (\omega, r^\ell_{\text{ne},2} + \lfloor \frac{q}{2} \rfloor),$$

for all inner knot values $\omega \in U_\ell \setminus \{0,1\}$, $\ell = 0,\dots,N$. The values $r^\ell_{\text{sw},2}$ and $r^\ell_{\text{ne},2}$ are defined in (7). Thus, the knot lines of the section curves extend over q knot spans with respect to V when considering odd degrees and $q+1$ knot spans for even degrees. The T-splines defined on this T-mesh are analysis-suitable since no horizontal T-junction extensions exist. Fig. 3 shows the T-mesh that defines the same basis as the patchwork hierarchy in Fig. 2.

Second, we construct a collection of LR B-splines, starting from a tensor-product mesh that possesses no inner knots in u-direction and a knot vector V as for the PB-splines. We perform meshline insertions with start point $(\omega, r^{\ell-1}_{\text{ne},2})$ and end point $(\omega, r^{\ell+1}_{\text{ne},2})$ for each inner knot $\omega \in U_\ell \setminus \{0,1\}$, for $\ell = 0,\dots,N$. The resulting mesh is the same that defines the patchwork hierarchy H. Note that the insertion of the meshlines can be formulated as a series of *primitive meshline extensions*, where we insert a new meshline spanning q elements and extend it $(q+1)$–times by a single element. Therefore, linear independence is guaranteed by the theory of LR B-splines, [6].

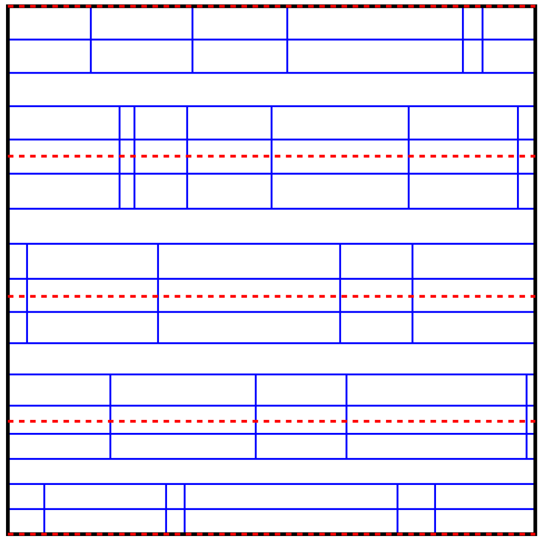

Fig. 3 Left: The T-mesh that defines the same basis as the patchwork hierarchy in Fig. 2.

Note that this equivalence with T-splines and LR B-splines is limited to the case of uniform degrees for all section curves, since these constructions do not support non-uniform degrees.

4.4 Constrained optimization

Theorem 5 guarantees that the patchwork spline space P contains at least one solution of the lofting problem. Uniqueness, however, is not guaranteed. We use numerical optimization to identify the 'best' solution.

In order to construct the PB-spline lofting surface we solve a constrained optimization problem where we minimize an energy term subject to the interpolation conditions,

$$\begin{aligned} \text{minimize} \quad & J(s) = \int_{\Omega} (\partial_{vv} s(u,v))^2 \\ \text{subject to} \quad & s(u,\bar{v}_k) = c_k(u), \quad \text{for all } k = 0,\ldots,N. \end{aligned}$$

On the patchwork hierarchy H, the interpolation conditions can be rewritten as

$$\sum_{j=k(q+1)}^{(k+1)(q+1)-1} c^k_{i,j} N_{j,q,V}(\bar{v}_k) = d_{i,k}, \quad \text{for all } i = 0,\ldots,m_k, \text{ and } k = 0,\ldots,N.$$

By using the method of Lagrange mutlipliers we obtain the system

$$\begin{pmatrix} E & B^T \\ B & 0 \end{pmatrix} \begin{pmatrix} c \\ \lambda \end{pmatrix} = \begin{pmatrix} 0 \\ d \end{pmatrix},$$

of linear equations, which is solved for the unknowns

$$c = (c^{\ell}_{i,j})_{\ell=0,\ldots,N;\,(i,j)\in\mathscr{K}^{\ell}}$$

and the Lagrange multipliers

$$\lambda = (\lambda_{i,k})_{k=0,\ldots,N;\,i=0,\ldots,m_k}.$$

The vector

$$d = (d_{i,k})_{k=0,\ldots,N;\,i=0,\ldots,m_k}$$

contains the control points of the given section curves. The $|K| \times |K|$ energy matrix E possesses the elements

$$e_{(\ell_1,i_1,j_1),(\ell_2,i_2,j_2)} = 2 \iint_{\Omega} N_{i_1,p_{\ell_1},U_{\ell_1}}(u) N_{i_2,p_{\ell_2},U_{\ell_2}}(u) \partial_{vv} N_{j_1,q,V}(v) \partial_{vv} N_{j_2,q,V}(v) du\, dv,$$

for $\ell_k = 0,\ldots,2N$ and $(i_k, j_k) \in \mathscr{K}^{\ell_k}$. The integrals in the above expression can be solved exactly by a Gaussian quadrature rule with $\lceil \frac{p+q-1}{2} \rceil$ points in each coordinate direction where $p = \max_{k=0,\ldots,N} p_k$. For the $(\sum_{k=0}^{N} m_k + 1) \times |K|$ constraints matrix B we obtain

$$b_{(\ell,i),(\ell,i,j)} = N_{j,q,V}(\bar{v}_{\ell}),$$

for $\ell = 0,\ldots,N$, $i = 0,\ldots,m_{\ell}$ and $(i, j) \in \mathscr{K}^{\ell}$. Note that the elements of B depend only on ℓ and j, therefore, $b_{(\ell,i_1),(\ell,i_1,j)} = b_{(\ell,i_2),(\ell,i_2,j)}$ for any $i_1, i_2 = 0,\ldots,m_{\ell}$.

5 Results

This section presents four lofting examples where we compare the results of using tensor-product B-splines with PB-splines. The blending-based lofting is not included, since the surface quality of this method is not satisfactory.

We start with two academic examples. In the first one, we consider curves of uniform degrees with highest order smoothness. For the second example, we use curves of varying degrees and knot multiplicities larger than 1. Furthermore, we present two real world examples, provided by our industrial partner MTU Aero Engines, where we construct a surface from a wireframe model consisting of 41 periodic curves with 153 control points each. In this case we use periodic PB-splines, which are straightforwardly obtained in the same way as periodic tensor-product B-splines.

We choose degree $q = 3$ for all examples.

First example

Consider the 21 section curves of uniform degrees $p_k = 3$ and maximum smoothness, which are shown in Fig. 4, left. The two lofting surfaces by tensor-product splines and PB-splines are virtually identical, and therefore we visualize only one of them, see Fig. 4, right. The maximum deviation between the surfaces $s_{\mathrm{tp}}(u,v)$ and $s_{\mathrm{pb}}(u,v)$ does not exceed $2.5e-4\%$ of the diameter of the bounding box. The tensor-product surface has $2,507$ (100%) control points, whereas the PB-spline surface needs only 756 (30.2%). Fig. 5 depicts the meshes in the parameteric domain for the tensor-product B-splines (left) and PB-splines (right), respectively. The knot lines of the tensor-product mesh extend over the entire unit square, while the patchwork hierarchy contains the knots of the curves only in a certain region around the associated parameter lines $v = \bar{v}_k$.

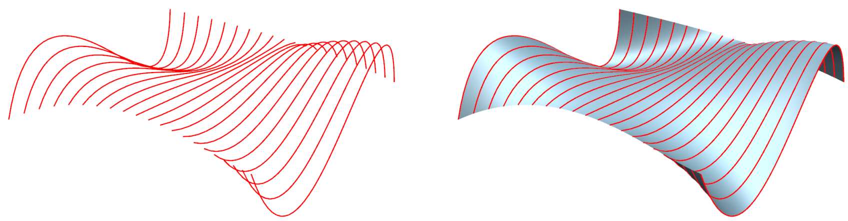

Fig. 4 Section curves and corresponding lofting surface $s_{\mathrm{pb}}(u,v)$ for the first example.

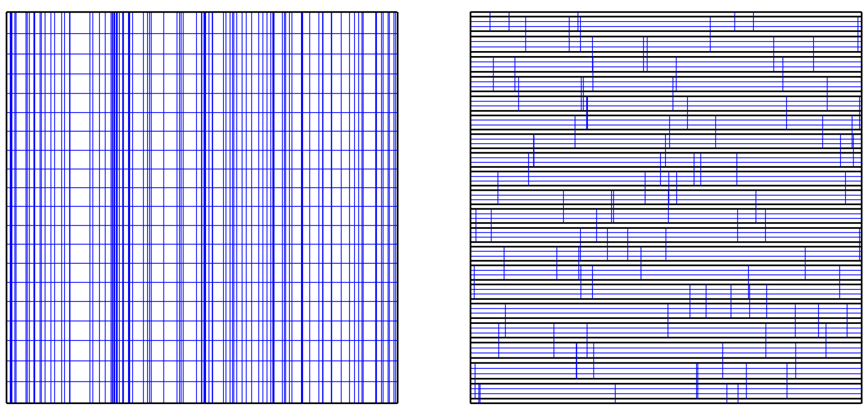

Fig. 5 2D meshes for tensor-product B-splines (*left*) and PB-splines (*right*). The black lines in the right picture represent the patch boundaries.

Second example

Consider the 11 section curves of varying degrees p_k between 2 and 4, see Fig. 6, left. Moreover, the knot vectors T_k contain knots with higher multiplicities, which even causes the loss of differentiability. In this case, the maximum deviation between the two results is smaller than 0.35% of the diameter of the bounding box. The tensor-product surface has $1,599$ (100%) control points, whereas the PB-spline surface needs only 508 (32%). Furthermore, the tangent discontinuities of the section curves extend to the entire tensor-product spline surface, while affecting only some patches of the PB-spline surface, see Fig. 7. The 2D meshes for both methods are illustrated in Fig. 8. Note that the different colors of the knot lines correspond to different orders of smoothness.

Third example

In the first industrial example we consider the wireframe model of a bulky airfoil with 41 periodic curves of degree 3 with maximum smoothness. Lofting with tensor-product B-splines requires $262,816$ (100%) control points. When using PB-splines we obtain a surface with only $24,600$ (9.4%) control points. The maximum deviation between the airfoils with a total height of 0.15m is 0.04μm. Fig. 10 shows the section curves on the left, followed by the lofting surface with reflection line analysis.

Fourth example

Example 4 is similar to the previous example. The only difference lies in the shape of the airfoil, which is rather thin and elongated. The tensor-product surface possesses $262,773$ (100%) control points, while the PB-spline surface is defined by $24,600$ (9.4%) control points. As before, the differences in the surfaces are marginal with a maximum deviation of 0.016μm for an airfoil height of 0.117m. Fig. 10 depicts the section curves and the lofting surface with reflection line analysis.

6 Conclusion

We applied the recently introduced framework of Patchwork B-splines (PB-splines) [3] to the construction of lofting surfaces. Especially, when considering a large number of section curves with many control points defined on disjoint knot vectors, the PB-splines offer a substantial advantage: The adaptivity of the PB-splines enables us to generate high-quality lofting surfaces with fewer control points compared to the standard tensor-product B-spline approach, where repeated global knot inser-

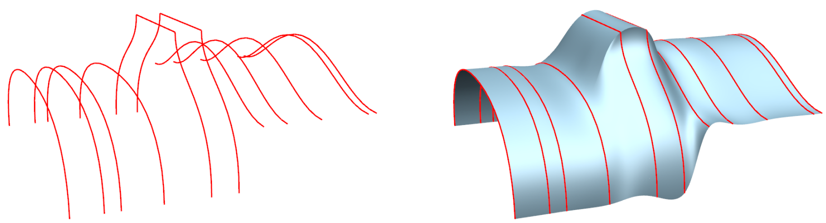

Fig. 6 Section curves and corresponding lofting surface $s_{pb}(u,v)$ for the second example.

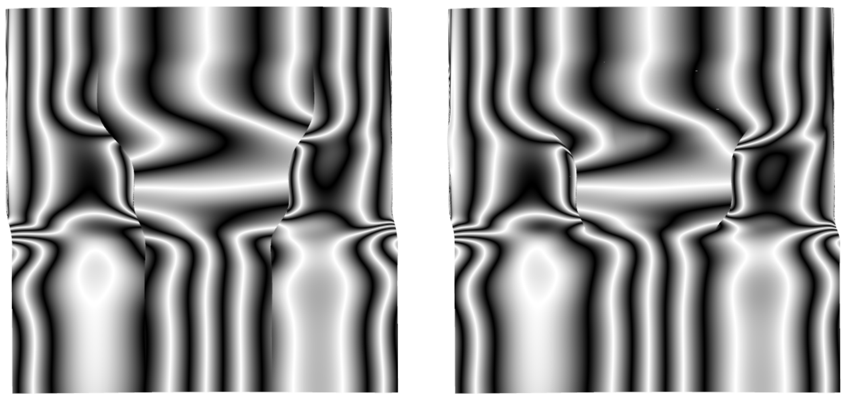

Fig. 7 Reflection lines on the tensor-product spline surface (*left*) and the PB-spline surface (*right*) illustrate the propagation of the tangential discontinuities.

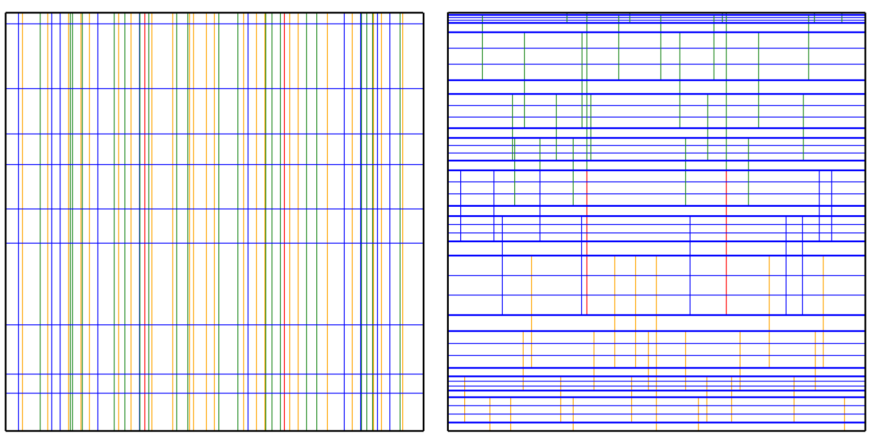

Fig. 8 2D meshes for tensor-product B-splines (*left*) and PB-splines (*right*) for the second example. The colors encode the degree of smoothness across knot lines, C^0 (*red*), C^1 (*orange*), C^2 (*blue*) and C^3 (*green*). Bold lines represent patch boundaries.

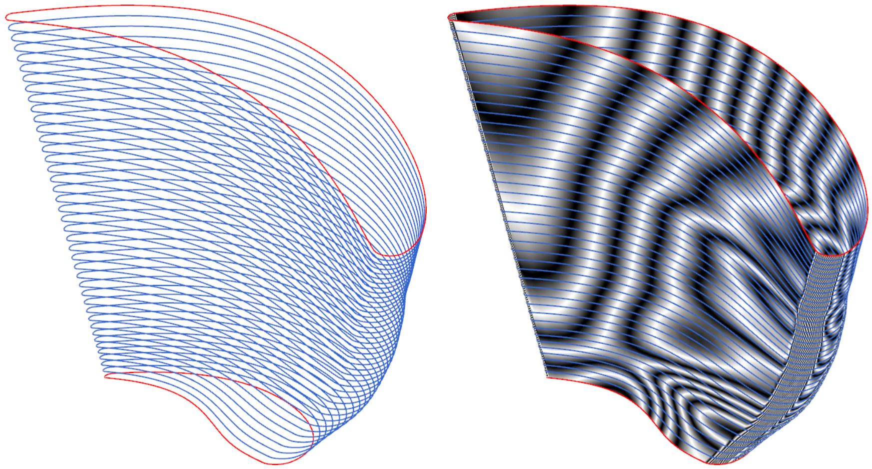

Fig. 9 Section curves and the resulting lofting surface with reflection lines for the third example.

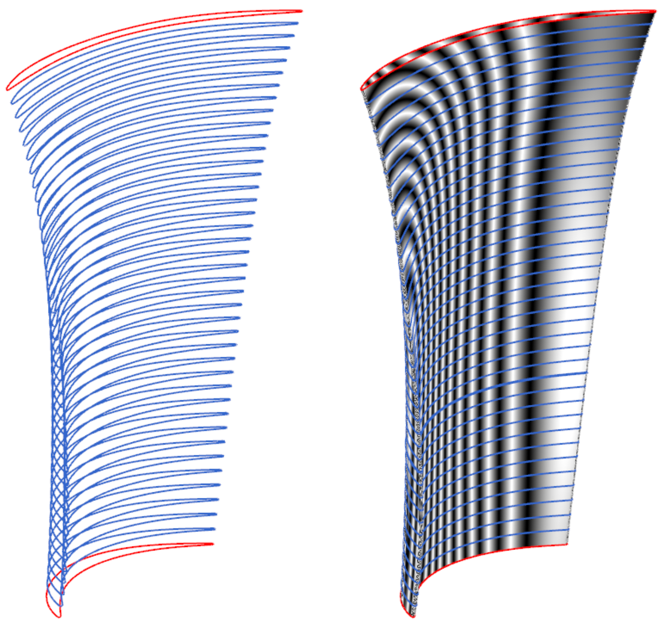

Fig. 10 Section curves and the resulting lofting surface with reflection lines for the fourth example.

tion is required. Moreover, the patchwork structure helps to limit the propagation of derivative discontinuities.

In contrast to the algorithms proposed in [10] and [15] the PB-spline lofting provides an exact interpolation of the section curves. Also, while [9] presents an algorithm for periodic cubic splines of C^0- and C^2-smoothness, we provide a very flexible method that works for arbitrary section curves. More precisely, these can be periodic, defined on knot vectors with varying multiplicites and possess different polynomial degrees. The use of an energy term, which was mentioned but not yet implemented in [9], leads to visually pleasing surfaces whithout bumps between the section curves.

Furthermore, a PB-spline surface can be exported as collections of standard tensor-product spline surfaces, thereby providing a simple way to use them in an existing CAD environment. The resulting model consists of $2N+1$ faces. Clearly, the built-in smoothness will not be preserved when performing additional control point modifications within CAD.

Finally, in the case of uniform degrees, we observed that the PB-splines used for constructing the lofting surface can equivalently be seen as analysis-suitable T-splines [13] or LR B-splines [2], defined by suitable meshes. The extension to non-uniform degrees, however, is not covered by these two existing constructions.

Acknowledgment

Supported by the Austrian Science Fund (FWF) though NFN S117 “Geometry + Simulation”. The authors thank MTU Aero Engines AG for kindly providing the airfoil data sets.

References

1. M. Bizzarri, M. Lávička, and J. Kosinka. Skinning and blending with rational envelope surfaces. *Computer Aided Design*, 87:41–51, 2017.
2. Tor Dokken, Tom Lyche, and Kjell Fredrik Pettersen. Polynomial splines over locally refined box-partitions. *Comput. Aided Geom. Des.*, 30(3):331–356, 2013.
3. N. Engleitner and B. Jüttler. Patchwork B-spline refinement. *Computer-Aided Design*, 90:168–179, 2017.
4. C. Giannelli, B. Jüttler, S.K. Kleiss, A. Mantzaflaris, B. Simeon, and J. Špeh. THB-splines: An effective mathematical technology for adaptive refinement in geometric design and isogeometric analysis. *Comp. Meth. Appl. Mech. Engrg.*, 299:337–365, 2016.
5. C. Giannelli, B. Jüttler, and H. Speleers. THB–splines: The truncated basis for hierarchical splines. *Computer Aided Geometric Design*, 29:485–498, 2012.
6. Kjetil Andr Johannessen, Trond Kvamsdal, and Tor Dokken. Isogeometric analysis using LR B-splines. *Computer Methods in Applied Mechanics and Engineering*, 269:471 – 514, 2014.
7. R. Kraft. *Adaptive und linear unabhängige Multilevel B-Splines und ihre Anwendungen*. PhD thesis, Univ. Stuttgart, 1998.

8. R. Kunkli and M. Hoffmann. Skinning of circles and spheres. *Computer Aided Geometric Design*, 27(8):611–621, 2010.
9. Y. Li, W. Chen, Y. Cai, A. Nasri, and J. Zheng. Surface skinning using periodic T-spline in semi-NURBS form. *J. Comput. Appl. Math.*, 273:116–131, 2015.
10. L. Piegl and W. Tiller. Algorithm for approximate NURBS skinning. *Computer-Aided Design*, 28:699–706, 1996.
11. L. Piegl and W. Tiller. *The NURBS Book*. Springer, New York, 2nd edition, 1997.
12. L. Piegl and W. Tiller. Surface skinning revisited. *The Visual Computer*, 18:273–283, 2002.
13. M.A. Scott, X. Li, T.W. Sederberg, and T.J.R. Hughes. Local refinement of analysis-suitable T-splines. *Computer Methods in Applied Mechanics and Engineering*, 213-216:206 – 222, 2012.
14. C.D. Woodward. Cross-sectional design of B-spline surfaces. *Computers and Graphics*, 11(2):193–201, 1987.
15. Y. Yang and J. Zheng. Approximate T-spline surface skinning. *Computer-Aided Design*, 44:1269–1276, 2012.